Monthly Notices of the ROYAL ASTRONOMICAL SOCIETY

MNRAS **519,** 902–908 (2023)
Advance Access publication 2022 December 08

https://doi.org/10.1093/mnras/stac3528

Spiral arms and the angular momentum gap in Milky Way Cepheids

Marcin Semczuk [1]★ Walter Dehnen [1,2] Ralph Schönrich [3] and E. Athanassoula[4]

[1]*School for Physics and Astronomy, University of Leicester, University Road, LE1 7RH Leicester, UK*
[2]*Astronomisches Recheninstitut, Zentrum für Astronomie der Universität Heidelberg, Mönchhofstraße 12–14, D-69120 Heidelberg, Germany*
[3]*Mullard Space Science Laboratory, University College London, Holmbury St. Mary, Dorking, Surrey RH5 6NT, UK*
[4]*Aix Marseille Université, CNRS, CNES, LAM, F-13388 Marseille Cedex 13, France*

Accepted 2022 November 28. Received 2022 November 28; in original form 2022 October 21

ABSTRACT

The angular momentum distribution of classical Cepheids in the outer Milky Way disc is bimodal with a gap at $L_{\rm gap} = 2950\,{\rm km\,s^{-1}}$ kpc, corresponding to $R = 13$ kpc, while no similar feature has been found in the general population of disc stars. We show that star formation in multiple spiral arm segments at the same azimuth leads to such multimodality that quickly dissolves and only shows in young stars. Unlike other explanations, such as a 1:1 orbital resonance with the Galactic bar, this also accounts for the observed steepening of the stellar warp at $L_{\rm gap}$, since the adjacent spiral arms represent different parts of the warped gas disc, and for the predominance of the gap at negative Galactic longitude ($\ell < 0^\circ$), since for complex spiral structure this mechanism is limited in azimuth. In this scenario, the gap is clearly present only in young stars, as observed, while most purely stellar dynamical origins would affect all disc populations, including older disc stars.

Key words: stars: variables: Cepheids – Galaxy: disc – Galaxy: kinematics and dynamics – Galaxy: structure – galaxies: spiral.

1 INTRODUCTION

Classical Cepheids (CCs) are pulsating stars and their well-defined period–luminosity relation makes them excellent distance indicators. With ages of the order of few hundred Myr, they are also quite young. These two characteristics make them ideal tracers of the structure of the young Galactic disc. For example, CCs have been used to map the Galactic stellar warp (Chen et al. 2019; Skowron et al. 2019) and to estimate its parameters (Lemasle et al. 2022).

For the spiral arms of the Milky Way (MW), the results are certainly less clear than for the warp. This can be said about all spiral tracers in the Galaxy. The main problem is our location within the disc, which limits the view to the far side and hampers our understanding of the global picture. Nevertheless, several authors (e.g. Majaess, Turner & Lane 2009; Veselova & Nikiforov 2020; Poggio et al. 2021; Lemasle et al. 2022) attempted to trace spiral arms with CCs and pointed to the coincidence of their spatial distribution with spiral arms defined in the literature by other tracers. The ages of CCs imply that they could have undergone up to one Galactic rotation near the solar circle since their formation, which limits their distance from the spiral arm in which they were born. This was noted by Skowron et al. (2019) who discussed a few scenarios in which the current distribution of CCs could have originated from one, two, or three separate interstellar medium (ISM) spiral arms.

The recent *Gaia* Data Release 3 of the Gaia Collaboration (2022, hereafter G22) combined proper motions from *Gaia* EDR3 (Lindegren et al. 2021) with line-of-sight velocities and distances from the CC period–luminosity relation of Ripepi et al. (2019, 2022) to obtain the 3D kinematics of MW CCs. Using these data, Drimmel et al. (2022, hereafter D22) analysed the radial dependences of the azimuthal velocity v_ϕ and the z component $L_z = Rv_\phi$ of angular momentum for the CCs younger than 200 Myr. They found that these quantities follow a tight relation with radius R, showing a gap or local minimum at $L_z \approx 2950\,{\rm km\ s^{-1}}$ kpc (see fig. 1 of D22 or the bottom panel of Fig. 3).

D22 discussed several possible explanations of this gap, focusing mostly on orbital resonances with the Galactic bar. Instead, in this paper we suggest an alternative and much simpler explanation, namely that the observed gap in angular momentum originates from a spatial gap between two thin spiral arms in the ISM where the CCs formed. We illustrate this idea with a simulated spiral galaxy.

This paper is structured as follows. In Section 2, we introduce the simulated galaxy and discuss its properties. In Section 3, we describe the phase-space gap found in the simulated galaxy and discuss its origin and its connection to the warp. Sections 4 and 5 discuss and summarize our findings, respectively.

2 THE SIMULATED GALAXY

We found a simulated galaxy with a similar gap in run TNG50-1 of the magnetohydrodynamical cosmological suite IllustrisTNG (Nelson et al. 2019; Pillepich et al. 2019). Baryonic (gas/star) particles in TNG50-1 have a typical mass of $8.5 \times 10^4\,{\rm M_\odot}$ and a gravitational softening of 288 pc, implying a resolution sufficiently high to model galactic structures, such as spiral arms, with some detail. Within its simulation volume of $(50\,{\rm Mpc})^3$, TNG50-1 has about 130 galaxies as massive as the MW (Pillepich et al. 2019).

Our example galaxy (ID = 546474 at redshift $z = 0$) is a barred spiral with a total mass of $5.7 \times 10^{11}\,{\rm M_\odot}$ within 100 kpc. Inside

★ E-mail: marcin.semczuk@yahoo.com

© The Author(s) 2022.
Published by Oxford University Press on behalf of Royal Astronomical Society. This is an Open Access article distributed under the terms of the Creative Commons Attribution License (http://creativecommons.org/licenses/by/4.0/), which permits unrestricted reuse, distribution, and reproduction in any medium, provided the original work is properly cited.

Downloaded from https://academic.oup.com/mnras/article/519/1/902/6884151 by University College London user on 03 March 2023

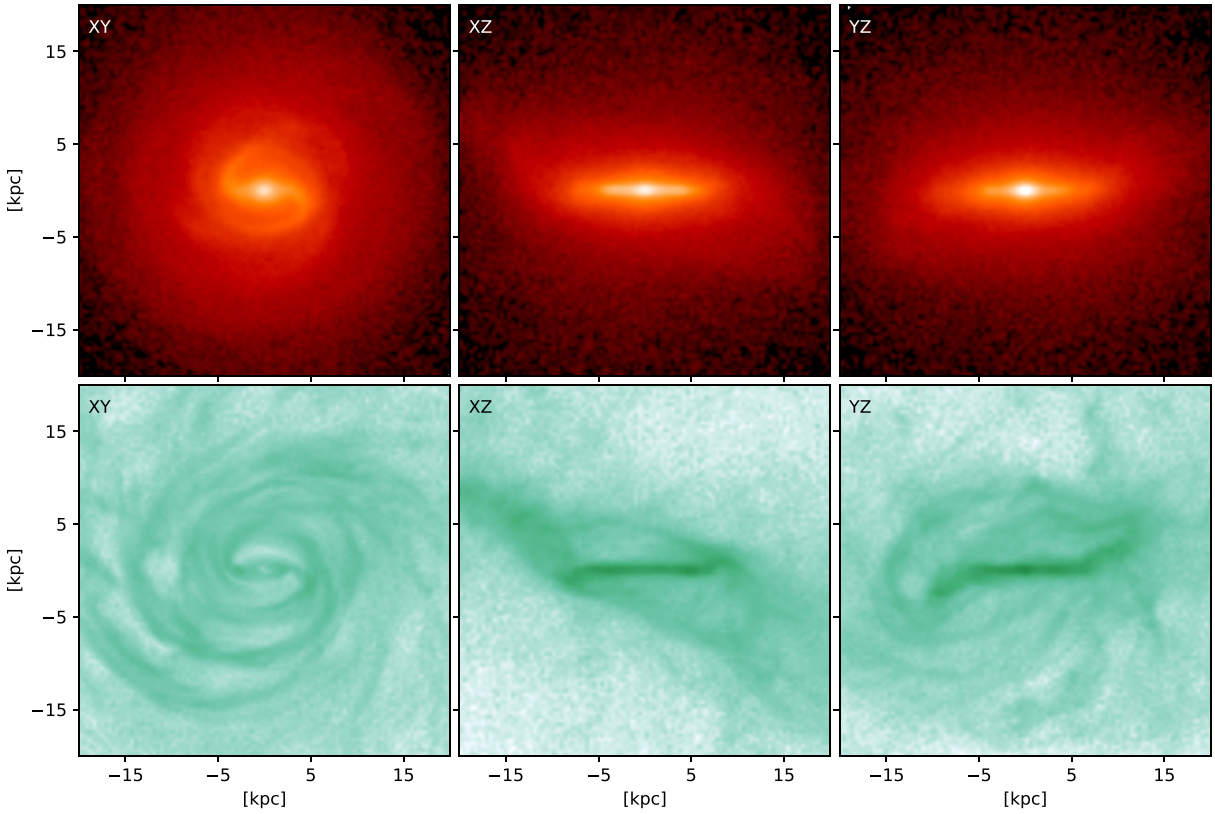

Figure 1. Density distribution of all stellar (top) and gas (bottom) particles of the simulated galaxy in three projections as indicated at redshift z = 0 (t = 13.803 Gyr).

20 kpc, the stellar and gas masses are 4.6×10^{10} and 1.4×10^{10} $M_\odot$, respectively, at $z = 0$. Most of the former are in an exponential disc with a scale length of 2.7 kpc. About 1 Gyr before the end of the simulation, a central bar formed and reached a radial extent of 3.3 kpc at $z = 0$. This bar rotates with a pattern speed of 34 km s^{-1} kpc^{-1} (obtained via the unbiased Fourier method of Dehnen, Semczuk & Schönrich 2023), which places co-rotation at 6.7 kpc, about twice the bar radius, implying a slow bar. The 2:1 bar resonance is at 10.8 kpc and 1:1 at 14.6 kpc.

Outside the bar region, the stellar and gaseous surface density maps of Fig. 1 show clear spiral structure, presumably due to tidal interactions. In the stellar disc, the spirals are much shorter and less pronounced than in the gas, where they are easily traceable to ∼3 times larger radii. The spiral structure in the stellar disc is dominated by an $m = 2$ mode, while gas spirals are more complex and multi-armed. The edge-on views show a strong warp, which again is more pronounced in the gas. This warp predates the bar, as it can be seen in the gas as early as 3 Gyr before the end of the simulation (not shown), and likely originates from misaligned gas accretion. More details on the evolution of the simulated galaxy can be found in Appendix A.

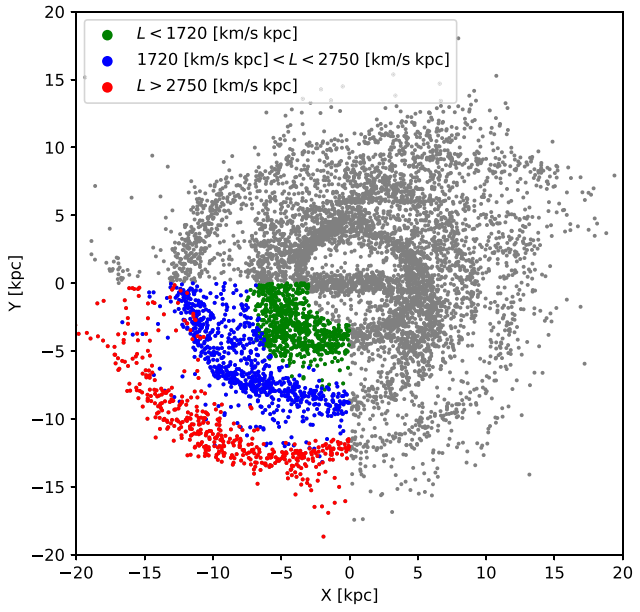

Figure 2. Spatial distribution of the stellar particles younger than 200 Myr from the simulated galaxy. Colour coded are three sub-samples separated by their angular momentum in the quadrant Q3 (see the third row of Fig. 3).

3 COMPARISON OF THE SIMULATION WITH THE MILKY WAY

3.1 Gap characterization

In order to emulate Galactic Cepheids, we select from the simulated galaxy star particles younger than 200 Myr, the same age limit as that used for CCs by D22 and G22. The face-on distribution of these particles, shown in Fig. 2, resembles more the gas morphology in Fig. 1 than the overall stellar distribution. Besides the bar and the spirals, these young stars also form a ring of the same size as the bar, i.e. a feature often observed in external galaxies and called an inner ring.

Downloaded from https://academic.oup.com/mnras/article/519/1/902/6884151 by University College London user on 03 March 2023

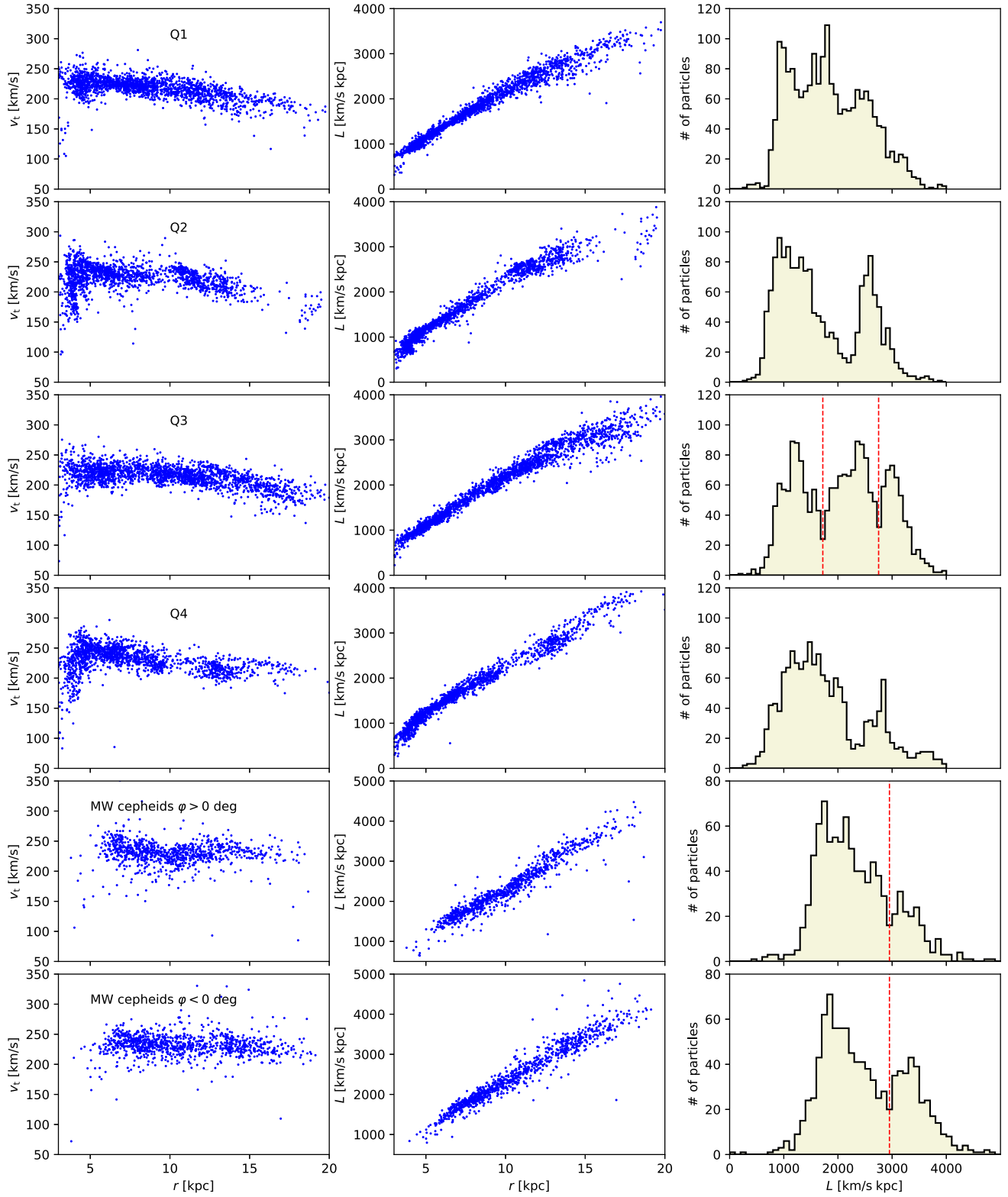

Figure 3. The distributions over spherical radius r and tangential velocity v_t (left) and total angular momentum $L = rv_t$ (middle), as well as histograms over L (right) for star particles at $r > 3$ kpc and younger than 200 Myr from each quadrant (as indicated; top four rows) of the simulated galaxy and for the MW CCs (bottom two rows) provided by G22 and D22 and split by their Galactic azimuth φ (defined to be zero at the Sun and increase towards Galactic rotation).

We divide these star particles by their azimuth into four quadrants in a reference frame aligned with the bar (other random orientations do not alter our results significantly; see Fig. 2) and do not consider particles from the inner 3 kpc, since G22 do not cover this inner region. In the first four rows of Fig. 3, we show for each quadrant the radial dependences of the tangential velocity v_t and the absolute value of the angular momentum L together with histograms of L for these young star particles. In the bottom two rows of Fig. 3, we show the

Downloaded from https://academic.oup.com/mnras/article/519/1/902/6884151 by University College London user on 03 March 2023

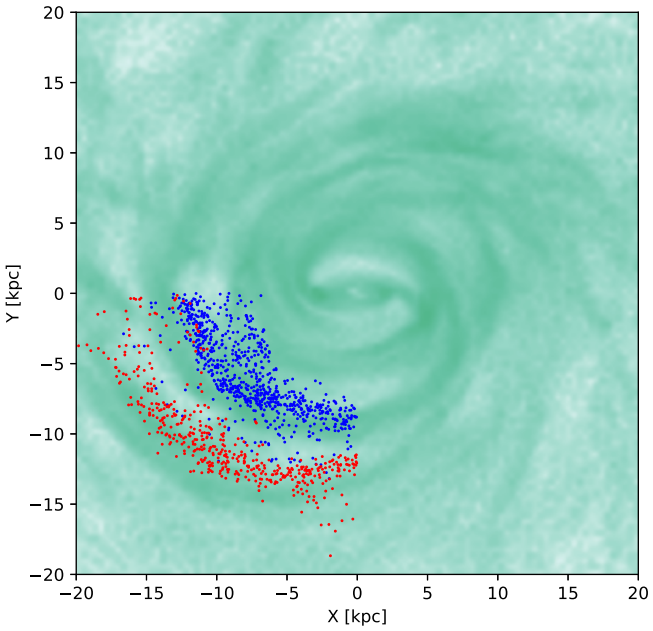

Figure 4. Face-on density distribution of the gas from the simulated galaxy with overlaid the scatter plot of the young stellar particles from the two spiral arms between which the angular momentum gap has formed. The selection of these particles is in Figs 2 and 3.

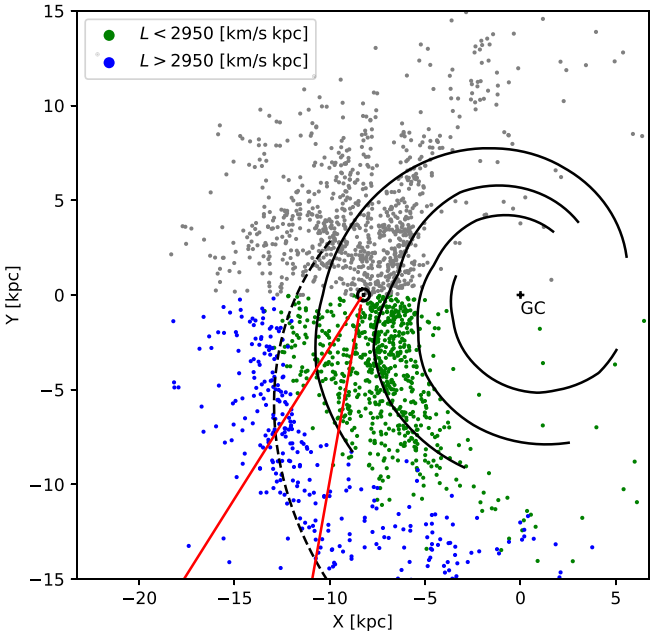

Figure 5. Spatial distribution of the Galactic classical Cepheids. Cepheids at $y < 0$ kpc (showing a clearer gap) are colour coded by their angular momentum. Solid and dashed black curves mark the four-arm spiral model of Taylor & Cordes (1993) and the Perseus arm (Levine, Blitz & Heiles 2006), respectively. Red lines indicate the region analysed in Fig. 8.

same quantities for the MW CCs obtained from G22 and D22[1] in two halves of the MW, split into positive and negative Galactic azimuth φ defined to be zero at Sun and increase towards Galactic rotation. We chose spherical radius r, v_t, and total angular momentum L here, instead of cylindrical radius R, v_ϕ, and L_z (as D22 did), in order to present a consistent comparison with the simulation. As discussed in Section 2, the disc of the simulated galaxy is strongly warped when v_ϕ and L_z capture the rotational motions only partly, while v_t and L provide the full picture. This change of variables hardly makes a difference for the distribution of MW CCs, as shown in fig. 1 of D22.

Angular momentum L shows tight relations with radius in each quadrant, slightly tighter in fact than MW CCs (which may be a consequence of errors in distance and/or radial velocity). For the MW CCs, the gap is more clearly visible at $\varphi < 0°$ (or $y < 0$ kpc), than at $\varphi > 0°$. In all quadrants of the simulated galaxy, the distributions have one or two gaps, most notable as dips in the histograms over L. The size and position of these gaps vary with azimuth corresponding to different arrangements of the spiral arms. Of all quadrants, Q3 best resembles the distributions of Galactic CCs at $\varphi < 0°$, except that it has not one but two clear gaps, the inner of which, at $L = 1720$ km s^{-1} kpc, has no analogue in the MW CC data.

We divide the young stellar particles from Q3 into three subsamples based only on their angular momentum L (as marked by dotted lines in Fig. 3) and paint them with different colour in the spatial map of Fig. 2. From this figure, it is clear that angular momentum separates stars into two spiral arms at different radii and an inner ring near the bar co-rotation radius. The obvious interpretation is that the gaps in angular momentum originate from the spatial gaps between the spiral arms in which these young particles actually formed. In Fig. 4, we overplot the young star particles associated with these two spirals on the gas density map viewed face-on. The star particles lie close to the gaseous spiral arms but slightly lag behind. This is expected because outside its co-rotation radius the spiral propagates faster than circular orbits and hence any stars (some evidence for this to also happen in MW was claimed by Hou & Han 2015). Unfortunately, the cadence of the TNG50 output data is insufficient to estimate the spiral pattern speed and co-rotation radius that would allow to investigate this in greater detail.

Ideally, we would present a plot similar to Fig. 2 or 4 for the MW. Unfortunately, this is not possible, because our inventory of MW CCs and our knowledge of the spiral structure in the MW gas disc are both incomplete. Instead, we compare in Fig. 5 the spatial distribution of CCs from our sample with the spiral-arm models from Taylor & Cordes (1993) and Levine et al. (2006). We see indeed that the CCs beyond the gap and at $y < 0$ kpc (blue) appear to align with the Perseus arm; inside the gap only the Sagittarius Carina (middle) arm is well sampled, while the other arms are barely distinguishable (both have been noted before by Poggio et al. 2021, G22).

3.2 Vertical structure

D22 noted that the L_z value of the gap in CCs coincides with the onset of the signal in vertical velocities v_z associated with the Galactic warp. If the gap is caused by some orbital resonance of the in-plane motions (such as an outer 1:1 resonance with the Galactic bar as favoured by D22), then such a coincidence is unexpected and indeed D22 concluded that its origin is unclear.

We investigate in Fig. 6 the vertical distributions of the groups of MW (bottom) and simulated (top) CCs separated by the angular momentum gaps. In both cases, the smallest L group (green) is vertically the narrowest and well confined to the galactic mid-plane,

[1]Deviating from G22, we used a solar velocity of 13, 250, and 6.9 km s^{-1} to translate to the Galactic frame, a blend of the results derived by Schönrich, Binney & Dehnen (2010) and Schönrich (2012).

Downloaded from https://academic.oup.com/mnras/article/519/1/902/6884151 by University College London user on 03 March 2023

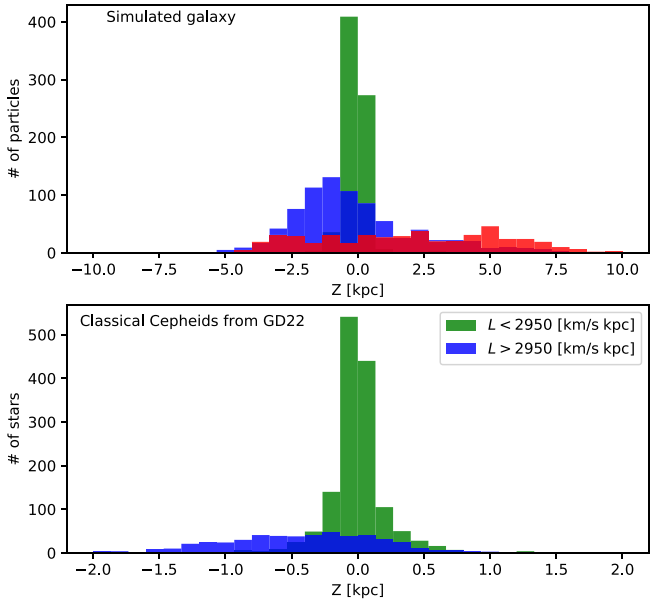

Figure 6. The distributions of the z coordinates for stellar particles from the simulated galaxy (top) and for Galactic classical Cepheids from the sample of D22 (bottom) for different subsets according to their total angular momentum L. The colour coding for the simulated galaxy is the same as in previous figures.

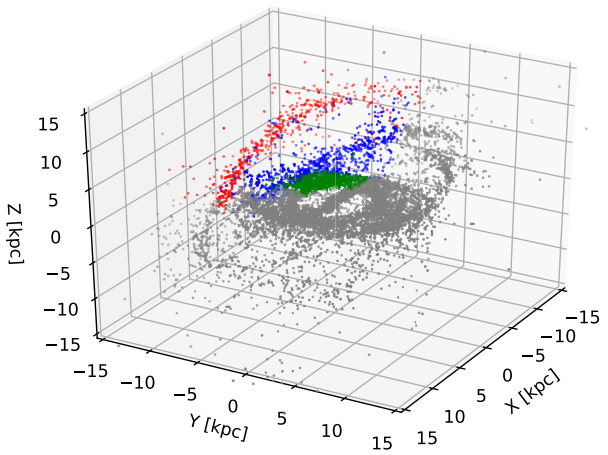

Figure 7. The 3D projection of the stellar particles younger than 200 Myr from the simulated galaxy. Colour coded are three sub-samples separated by their angular momentum in the quadrant Q3 (see the third row of Fig. 3). The projection demonstrates the origin of the vertical separation between the warped spiral arms.

while the groups beyond the respective gaps have very different vertical distributions: much broader and asymmetric.

For the simulated galaxy, Fig. 7 presents a 3D projection of the disc of young stars. Quite obviously, the outer spiral arm (red) is strongly warped with respect to the inner ring (green), which is almost aligned with the galactic plane, while the intermediate arm (blue) is intermediately warped between these. So with increasing L, the disc of young stars is increasingly warped, reflecting the state of the gas disc at the time of their birth. The same explanation likely holds for the MW CCs, albeit with a much weaker warp: the outer spiral beyond the gap was (at the time of forming the CCs) more inclined to the inner Galactic disc and gave birth to stars on correspondingly inclined orbits.

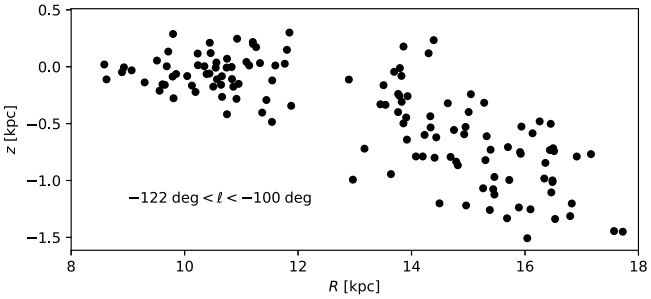

Figure 8. Distribution of Galactic cylindrical radius R and height z for Cepheids in the longitude range (highlighted by red lines in Fig. 5), where the biggest spatial gap occurs. If dust attenuation was responsible for the gap at $R = 12$–13 kpc, there should be no stars at $z \sim 0$ kpc and $R > 13$ kpc.

4 DISCUSSION

D22 review several possible explanations of the CC angular momentum gap. They dismiss a spiral-arm origin since the gap feature is present in not only the quadrant in which Poggio et al. (2021) identified the main spiral arm. Tracking spiral arms of the MW is traditionally a very difficult task, but we think that the origin from two adjacent spirals at the same azimuth can work even if these arms do not fully cover the same range of azimuths. For example, in Fig. 2 the red arm could end half way of its current azimuth range and the phase space would still show the gap. The only necessary condition for this mechanism to create a gap is to have two separated star-forming spiral arms in some azimuthal range.

D22 also consider a scenario in which the interaction with the Sgr Dwarf Galaxy punches a hole in the MW stellar disc that later winds up as a spiral with gaps (Bland-Hawthorn & Tepper-García 2021), but dismiss this scenario, since any passage of Sgr dwarf was far outside the location of the gap. In our scenario, however, such a wide interaction is welcome, as it may trigger a grand-design spiral in the gas disc well inside the actual passage, such as for M51. In fact, the simulated galaxy underwent two similar interactions (objects of $\sim 10^8$ $M_\odot$ passing within ~ 20 kpc), which may be responsible for the grand-design spiral pattern that later caused the angular momentum gaps in the young stars.

A close inspection of Fig. 5 suggests that the signal for the angular momentum gap in Fig. 3 is dominated by a relatively small region in the disc at Galactic longitudes $-100^\circ < \ell < -122^\circ$ (highlighted by red lines in Fig. 5). One might suspect this to result from dust attenuation hiding mid-plane stars until the warp brings them back out of the shadow. To test this, we plot in Fig. 8 the distribution of the MW CCs in R and z in that longitude range. While most stars beyond the gap are well below the Galactic mid-plane due to warp (as analysed from MW CCs by Lemasle et al. 2022), some very close to $z = 0$ kpc should not be visible if dust attenuation caused the angular momentum gap (in this segment).

Another obvious explanation for any gaps in phase space is some orbital resonance with a regular non-axisymmetric perturber, in particular the Galactic bar. A prediction of non-linear perturbation theory is that a stationary bar, or spiral pattern, may drive a warp outside its outer 2:1 (Lindblad) resonance (OLR; Masset & Tagger 1997). While the angular momentum gap at $R \approx 13$ kpc indeed coincides with the steepening of the Galactic warp, it is outside the OLR of the bar. D22 therefore considered the outer 1:1 resonance

Downloaded from https://academic.oup.com/mnras/article/519/1/902/6884151 by University College London user on 03 March 2023

with the bar, which is expected at that location, but could not find convincing evidence for a similarly clear gap in any other tracer, including millions of stars from the *Gaia* radial-velocity sample and a red giant branch sample (both with 6D phase-space information). This essentially rules out such an explanation, since resonance mechanisms differentiate stellar populations based on their velocity dispersion, and hence should affect all disc populations, albeit more so those with lower velocity dispersion. However, this remains unexplored for evolving resonances, in particular a slowing bar that drives some age discrimination (Chiba & Schönrich 2021).

Our proposed scenario, on the other hand, differentiates directly on stellar age, strongly favouring young stars, since (i) it requires a special configuration of their birth places, which may not exist for extended periods of time, and (ii) the feature gets quickly erased by phase mixing and angular momentum dispersal due to spiral and bar perturbations. In the simulated galaxy, for example, we find that gaps in the angular momentum distributions can be easily detectable only for stellar particles younger than about 1 Gyr. However, as we find in the simulated galaxy, the older stellar population may have features (such as ridges) at a similar phase-space position, which are unrelated and likely formed by interactions with some perturber (bar, spiral, or satellite).

It has been widely studied that the interaction between the MW and the Sgr Dwarf Galaxy could have created a warp (e.g. Ibata & Razoumov 1998), a corrugation (e.g. Gómez et al. 2013; Laporte et al. 2018), the phase-space spiral (e.g. Binney & Schönrich 2018; Laporte et al. 2019), and spiral arms (e.g. Purcell et al. 2011) in the MW stellar disc. It would have been surprising if only the vertical structure of the stellar and gas disc are affected by such an interaction, and the horizontal structure remained unaffected. Unfortunately, owing to the difficulty of obtaining the distance of H I emitting gas, observational evidence for the MW gaseous spiral arms is quite limited (Koo et al. 2017). An alternative, albeit possibly distorted, snapshot of the gas disc is provided by the young stars like CCs.

5 SUMMARY

We present an explanation for the gap at $L_{\rm gap} = 2950\,{\rm km\ s^{-1}\,kpc}$, corresponding to $R = 13$ kpc, found in the distribution of the angular momenta L of MW CCs (D22; see Fig. 3) and illustrate it with a simulated galaxy from IllustrisTNG run TNG50-1. The simulated galaxy has an extended spiral structure that is traced by both the gas and the stars corresponding in age to the MW CCs. The distributions of these young star particles over radius, tangential velocity, and angular momentum resemble those for the MW CCs. In particular, their distributions over L are multimodal in all quadrants with at least one clear gap, caused by a spatial gap between their birth places in two spiral arms at the same azimuth. While the precise formation mechanism for these spirals cannot be extracted from the TNG50 run (owing to the low output cadence), the recent close flybys of two $\sim 10^8\,{\rm M_\odot}$ objects within ∼20 kpc of the simulated galaxy are likely to have played a role.

For this same mechanism to be the origin of the gap found in the MW CCs, two spiral arms on either side of $R = 13$ kpc must have formed stars 100–200 Myr ago. While tracing the spiral structure of the Galactic ISM is notoriously difficult, the MW is not short of massive perturbers, such as the Sgr dwarf galaxy, which could have triggered or enhanced the spiral structure in the outer Galactic disc, leading to the formation of two spiral arms at the same azimuth and in the required radial range.

This explanation implies several properties, all of which are readily testable and in fact present. First, the angular momentum gap at this position is *only* present in populations of young stars, whose phase-space distribution still reflects their birth places. For older stars, phase mixing together with bar and spiral perturbations quickly erases any coherence from a common origin. The precise age beyond which this feature should disappear is hard to predict, but based on the simulated galaxy we expect it to be around 1 Gyr. The absence of a similar and clear phase-space feature in the general stellar disc (D22) therefore corroborates our explanation and largely excludes a purely dynamical origin, such as orbital resonances with the Galactic bar, which affects all disc stars to some degree, depending on their velocity dispersion.

A second property is that the gap may coincide with some discontinuity in the properties of the warp, because two spirals in different parts of the warped gas discs will have distinct orbital planes. This is the case in the simulated galaxy, which has a strong warp, but also for the MW CCs, where the gap visibly separates the stars in two populations in z.

Finally, as seen in the simulated galaxy, the same angular momentum gap is limited to some azimuthal range: the spiral arms giving birth to Cepheids have sufficient radial separation, but shift in radius with azimuth. This latter property is in fact reflected in the distribution of MW CCs, which show the gap being more pronounced at negative Galactic azimuth.

ACKNOWLEDGEMENTS

We are grateful to R. Drimmel and S. Khanna for providing the ages and distances of CCs from G22, to the IllustrisTNG team for making their simulations publicly available, and to the anonymous reviewer for a prompt report. We appreciate insightful discussions with Hossam Aly and Ewa L. Łokas. This work was supported by STFC grant ST/S000453/1. MS thanks B.-E. Semczuk for support. EA thanks the CNES for financial support. RS thanks the Royal Society for generous support via a University Research Fellowship.

DATA AVAILABILITY

No data were generated in this study.

REFERENCES

Binney J., Schönrich R., 2018, MNRAS, 481, 1501
Bland-Hawthorn J., Tepper-García T., 2021, MNRAS, 504, 3168
Chen X., Wang S., Deng L., de Grijs R., Liu C., Tian H., 2019, Nat. Astron., 3, 320
Chiba R., Schönrich R., 2021, MNRAS, 505, 2412
Dehnen W., Semczuk M., Schönrich R., 2023, MNRAS, 518, 2712
del Pino A., Fardal M. A., van der Marel R. P., Łokas E. L., Mateu C., Sohn S. T., 2021, ApJ, 908, 244
Drimmel R. et al., 2022, accepted for publication in A&A, preprint (arXiv:2207.12977) (D22)
Gaia Collaboration, 2022, A&A, in press, preprint (arXiv:2206.06207) (G22)
Gómez F. A., Minchev I., O'Shea B. W., Beers T. C., Bullock J. S., Purcell C. W., 2013, MNRAS, 429, 159
Hou L. G., Han J. L., 2015, MNRAS, 454, 626
Ibata R. A., Razoumov A. O., 1998, A&A, 336, 130
Koo B.-C., Park G., Kim W.-T., Lee M. G., Balser D. S., Wenger T. V., 2017, PASP, 129, 094102
Laporte C. F. P., Johnston K. V., Gómez F. A., Garavito-Camargo N., Besla G., 2018, MNRAS, 481, 286
Laporte C. F. P., Minchev I., Johnston K. V., Gómez F. A., 2019, MNRAS, 485, 3134
Lemasle B. et al., 2022, A&A, 668, 40
Levine E. S., Blitz L., Heiles C., 2006, Science, 312, 1773

Downloaded from https://academic.oup.com/mnras/article/519/1/902/6884151 by University College London user on 03 March 2023

Lindegren L. et al., 2021, A&A, 649, A2
Majaess D. J., Turner D. G., Lane D. J., 2009, MNRAS, 398, 263
Masset F., Tagger M., 1997, A&A, 318, 747
Nelson D. et al., 2019, MNRAS, 490, 3234
Pettitt A. R., Tasker E. J., Wadsley J. W., 2016, MNRAS, 458, 3990
Pillepich A. et al., 2019, MNRAS, 490, 3196
Poggio E. et al., 2021, A&A, 651, A104
Purcell C. W., Bullock J. S., Tollerud E. J., Rocha M., Chakrabarti S., 2011, Nature, 477, 301
Ripepi V., Molinaro R., Musella I., Marconi M., Leccia S., Eyer L., 2019, A&A, 625, A14
Ripepi V. et al., 2022, A&A, 659, A167
Schönrich R., 2012, MNRAS, 427, 274
Schönrich R., Binney J., Dehnen W., 2010, MNRAS, 403, 1829
Skowron D. M. et al., 2019, Science, 365, 478
Taylor J. H., Cordes J. M., 1993, ApJ, 411, 674
Vasiliev E., Belokurov V., Erkal D., 2021, MNRAS, 501, 2279
Veselova A. V., Nikiforov I., 2020, Res. Astron. Astrophys., 20, 209
Wang H.-F., Yang Y.-B., Hammer F., Wang J.-L., 2022, preprint (arXiv:2204.08542)

APPENDIX A: EVOLUTION OF THE SIMULATED GALAXY

Over the past 3–4 Gyr, the simulated galaxy experienced several mild tidal interactions from flybys of smaller objects. At $t = 12.8$ Gyr, the time of bar formation, for example, two sub-haloes with total masses of 10^9 and 5×10^8 $M_\odot$, respectively, passed within about 30 and 20 kpc from the galactic centre. These interactions might have induced the bar and $m = 2$ spirals (we cannot ascertain this from the low-cadence output of TNG50). Fig. A1 presents the snapshots of the face-on surface density of the stellar and gaseous discs in the last 680 Myr, showing vivid evolution of the $m = 2$ stellar spiral, whose asymmetric nature (e.g. at $t = 13.328$ Gyr) suggests a tidal origin. The grand-design spiral in the last snapshot, which we analysed in detail, might have been induced by the close (∼20 kpc) preceding passages of two light sub-haloes of 1.2×10^8 and 0.4×10^8 $M_\odot$, respectively. While their masses are below the limits for spiral-arms induction suggested by idealized simulations (Pettitt, Tasker & Wadsley 2016), SUBFIND might slightly underestimate these masses of objects already embedded in the main halo. The near-simultaneous passages of two separate sub-haloes can interfere in constructive (or destructive) ways. Owing to the presence of mild interactions and other processes that could possible affect the morphology, such as misaligned gas accretion, we cannot determine the precise formation mechanism of the spirals with any certainty without re-simulating the past 2 Gyr in isolation. Nevertheless, it seems likely that the MW exhibited stronger tides from its satellites. For Sagittarius, for example, the initial mass ranges from 0.9×10^9 to 3.8×10^9 $M_\odot$ with last pericentres ∼20 kpc varying between different models (e.g. del Pino et al. 2021; Vasiliev, Belokurov & Erkal 2021; Wang et al. 2022).

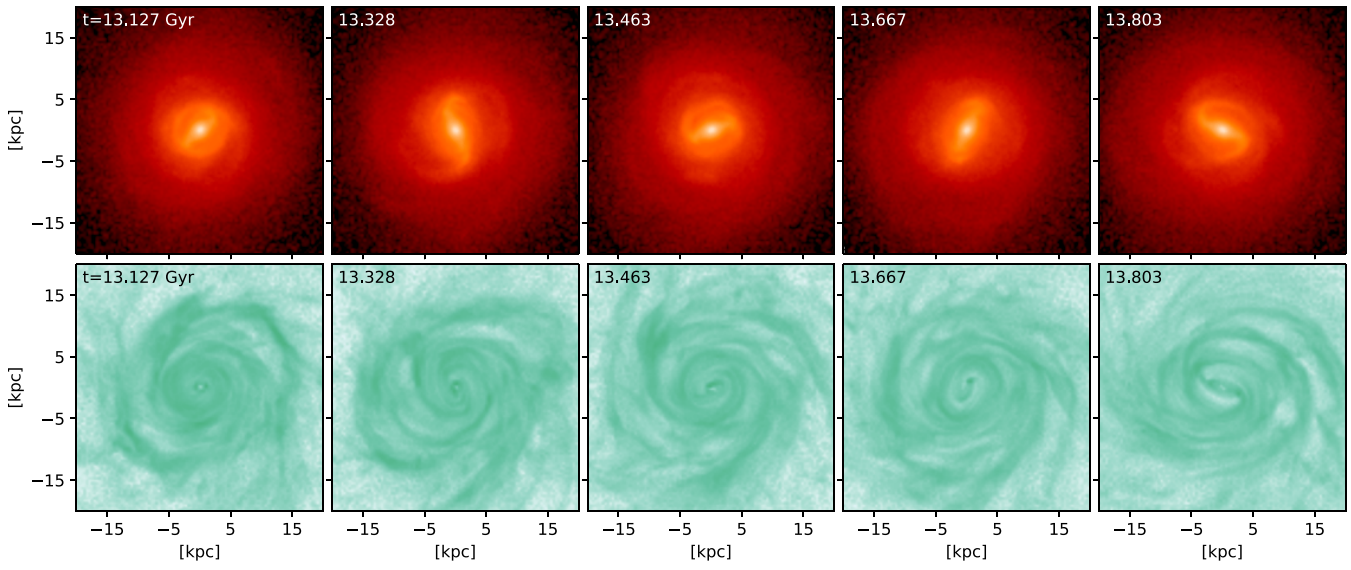

Figure A1. Face-on surface density distribution of all star (top) and gas (bottom) particles of the simulated galaxy for the last five snapshots, demonstrating the recent evolution of spiral structure.

This paper has been typeset from a TEX/LATEX file prepared by the author.

Downloaded from https://academic.oup.com/mnras/article/519/1/902/6884151 by University College London user on 03 March 2023